

## Accepted Manuscript

Title: Methanol assisted methane conversion for higher hydrocarbon over bifunctional Zn-modified Mo/HZSM-5 catalyst

Author: Sachchit Majhi Ajay. K Dalai Kamal K Pant



PII: S1381-1169(14)00579-2  
DOI: <http://dx.doi.org/doi:10.1016/j.molcata.2014.12.019>  
Reference: MOLCAA 9381

To appear in: *Journal of Molecular Catalysis A: Chemical*

Received date: 16-9-2012  
Revised date: 24-12-2014  
Accepted date: 27-12-2014

Please cite this article as: Sachchit Majhi, Ajay.K Dalai, Kamal K Pant, Methanol assisted methane conversion for higher hydrocarbon over bifunctional Zn-modified Mo/HZSM-5 catalyst, Journal of Molecular Catalysis A: Chemical <http://dx.doi.org/10.1016/j.molcata.2014.12.019>

This is a PDF file of an unedited manuscript that has been accepted for publication. As a service to our customers we are providing this early version of the manuscript. The manuscript will undergo copyediting, typesetting, and review of the resulting proof before it is published in its final form. Please note that during the production process errors may be discovered which could affect the content, and all legal disclaimers that apply to the journal pertain.

**Methanol assisted methane conversion for higher hydrocarbon over bifunctional Zn-modified Mo/HZSM-5 catalyst**

*Sachchit Majhi<sup>ab</sup>, Ajay. K Dalai<sup>b</sup>, Kamal K Pant<sup>a\*</sup>*

<sup>a</sup>Department of Chemical Engineering, Indian Institute of Technology Delhi, Hauz Khas, New Delhi 110016, India

<sup>b</sup>Department of Chemical and Biological Engineering, University of Saskatchewan, Saskatoon, SK S7N 5C5, Canada

Highlights

- Novel Zn-Mo/HZSM-5 catalyst was prepared for methane conversion with methanol.
- The change in textural properties, and product selectivity, were investigated with Zn addition.
- Incorporation of Zn increased the conversion and aromatic selectivity.

**Abstract**

The co-conversion of methane with methanol was studied over Mo/H-ZSM-5 and Zn-Mo/H-ZSM-5 catalysts prepared by the wet impregnation method. The catalysts were calcined at 550 °C followed by reduction at 450 °C for 5h. The activity tests were carried out at three different temperature viz. 550, 600, and 650°C. BET, BJH pore volume distribution, H<sub>2</sub>-TPR, NH<sub>3</sub>-TPD, FTIR, SEM-EDX, TEM, and XRD techniques were used for the characterization of the pre-reduced catalyst. Incorporation of 2%Zn on to 5%Mo/H-ZSM-5 catalyst significantly improved the activity of the catalyst for methane conversion. Thermodynamic studies revealed that temperature below 600 °C, methane aromatization is not possible, however in the presence of methanol over bifunctional catalyst it becomes thermodynamic feasible ( $\Delta G = -8.8, -15.5, \text{ and } -22.2 \text{ kJ/mol}$  at 400, 500, and 600 °C). The main products of the reaction were ethylene, ethane, propane,

butane butylenes and aromatics such as benzene, toluene, ethyl benzene and xylene. Selectivity of alkylated aromatic product enhance in the presence of methanol.

**Keywords:** Co-conversion; HZSM-5; Bifunctional catalyst; Additives; Aromatics; Reaction mechanism

---

\*Corresponding author

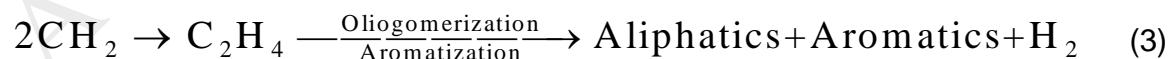
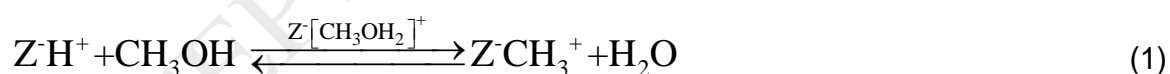
Email: [kkpant@chemical.iitd.ac.in](mailto:kkpant@chemical.iitd.ac.in); Tel.: +91 11 26596177; Fax: +91 11 26596172

## 1.0 Introduction:

With the increased demand for energy worldwide and the limited worldwide availabilities of crude oil reserves have led to exorbitantly high crude oil prices. The abundance of natural gas worldwide has drawn much attention toward its effective utilization as fuel. The reserves of natural gas are located in remote areas where high transport costs affect exploitation; however, by adopting procedures for the conversion of natural gas to higher hydrocarbons these costs can be reduced [1]. Efforts are being made to convert methane into high-density liquid fuel by various researchers in industry and academia [2]. Methane can be converted to higher hydrocarbon by mainly two routes: indirect and direct methods. The indirect route for methane conversion (e.g., Fischer-Tropsch, Mobil Process, and Shell Middle Distillate Synthesis) requires the production of synthesis gas (CO and H<sub>2</sub>) from methane by the costly and inefficient process of steam reforming [3]. The direct route of methane conversion to higher hydrocarbons has attracted researchers, due to its potential for utilizing natural gas as industrial feedstock. However, the usefulness of this process is still limited as it has not been possible to achieve large-scale conversion of methane directly to higher hydrocarbons. Owing to its stable configuration of four symmetric C-H bonds having

bond energy of 435 kJ/mol it is not feasible at low temperatures whereas at high temperature the tendency of coke deposition on the active surface also increases. In order to suppress coking with reasonably high conversion, additives such as alkanes or alcohols are required in the reactant stream to activate the methane molecule at low temperatures [4-7]. Thermodynamically; methane is unstable only above 530 °C, becoming more unstable than benzene above 1030 °C [3]. The equilibrium methane conversion at atmospheric pressure is low at moderate temperatures (about 5% at 600 °C, 11.4% at 700 °C and 16.2% at 750 °C) [5]. For the case of methane methanol simultaneous conversion,  $\Delta G = -8.8, -15.5,$  and  $-22.2 \text{ kJmol}^{-1}$  at 400, 500, and 600 °C, respectively, for one mole of methane converted per mole of methanol (Co-conversion of methane with methanol to benzene) [7]. The methanol to gasoline (MTG) is a highly exothermic reaction ( $\Delta H_r = -1670 \text{ kJ/kg}$ ); whereas, methane conversion is an endothermic process. The present work examines a combination of the exothermic conversion of methanol with the highly endothermic methane cracking reaction to obtain relatively thermo neutral reaction.

The probable reaction mechanisms of the methane-methanol reaction can be understood by the following mechanism:





Where  $\text{H}^+\text{Z}^-$  =HZSM-5,  $\text{M}^{n+}$  = Mo or Zn oxide

Among the several catalysts tested, Mo/HZSM-5 has been reported the most promising catalyst [8, 9, 10, 11]. This could be due to its framework of HZSM-5 and active sites located in cavities or channels of the zeolite pore system, which is predetermined by their structural nature, particularly the shape and size of pores. Thus, the accessibility of sites and nature of the products formed during the reaction is controlled by zeolite [12, 13]. Having a two-dimensional porous structure and pore diameter close to the dynamic diameter of the benzene molecule, HZSM-5 as support for the aromatization of methane inhibition effectively ensures the formation of other products [14]. To modify the activity of the catalyst, the addition of a metal promoter was implemented, enhancing the catalytic activity and selectivity to benzene and other hydrocarbons [15].

In this work, a relatively thermo-neutral reaction by means of methanol as a co-reactant over the catalysts, namely 5%Mo/HZSM-5 and 5%Mo-2%Zn/HZSM-5, prepared by the impregnation method was studied. These catalysts were characterized by BET surface area, pore volume, BJH adsorption-desorption, and temperature programmed reaction (TPR) method. The acidity measurements of the calcined catalyst were conducted by FTIR and temperature programmed desorption (TPD) using  $\text{NH}_3$ . The surface morphology was analyzed by SEM-EDX and TEM analyses. The percentage coke formed during the reaction was determined by TGA. The activity tests

of these catalysts were performed in a quartz reactor over the temperature range of 550 to 650°C at atmospheric pressure.

## 2.0 Experimental

### 2.1 Catalyst Preparation

The chemicals used were  $(\text{NH}_4)_6\text{Mo}_7\text{O}_{24}\cdot 4\text{H}_2\text{O}$  (Merck, Germany) and  $\text{Zn}(\text{NO}_3)_2\cdot 6\text{H}_2\text{O}$  (Merck, India) as the metal precursor. Commercial HZSM-5 was supplied by Sud-chemie, having a silica alumina ratio of 55. Two catalysts were prepared by impregnation over an HZSM-5 support. The first catalyst, 5.0% Mo/HZSM-5 (ascribed as CAT-1), was prepared by impregnation with an aqueous solution of ammonium heptamolybdate  $[(\text{NH}_4)_6\text{Mo}_7\text{O}_{24}\cdot \text{H}_2\text{O}]$  over HZSM-5 zeolite. After impregnation, the catalyst was dried at  $110\pm 5^\circ\text{C}$  overnight and then calcined in air at  $550\pm 5^\circ\text{C}$  for 5 h. The second catalyst, 2% Zn-5% Mo/HZSM-5 (ascribed as CAT-2), was prepared by impregnation on HZSM-5 with ammonium heptmolybdate and a  $\text{Zn}(\text{NO}_3)_2\cdot 6\text{H}_2\text{O}$  solution. The subsequent steps were the same as for CAT-1.

### 2.2 Catalyst Characterization

The textural properties of the catalyst and adsorption-desorption isotherms were determined using nitrogen and a Micromeritics ASAP 2010 apparatus. For the cross-sectional area of  $\text{N}_2$ , a value of  $0.162\text{ nm}^2$  was used. Prior to the experiments, the samples were degassed at  $150^\circ\text{C}$  in the vacuum condition for 3 h to remove moisture and gases. Micropore distributions were derived from the Horvath-Kawazoe (HK) method; whereas, mesopore distributions were derived from the Barrett-Joyner-Halenda

(BJH) method. Surface areas and pore volumes of the catalyst samples were measured with the BET method.

The temperature program reduction (TPR) study was done to determine the reduction temperature using a Micrometrics Pulse Chemisorb 2720 apparatus. Approximately 0.1 g of the sample was taken in a U-type quartz tube and then reduced from ambient to 950°C at a ramp rate of 10°C/min, under a hydrogen-argon mixture (10% hydrogen), at a flow rate of 20 ml/min. The hydrogen consumption during the TPR was recorded by means of a thermal conductivity detector (TCD). The acidity of the HZSM-5 and metal loaded HZSM-5 catalysts were measured by temperature programmed desorption (TPD) of ammonia using the same equipment. For this 0.2 g of catalyst sample was pretreated in a flow of helium at 500°C for 1 h to remove moisture present in the sample and then cooled down to room temperature. To complete saturation, an ammonia-helium mixture (5:95) was passed to the sample for 1 h. Physisorbed ammonia was removed by flowing helium for 30 min. After that, TPD was carried out in a stream of helium with a flow rate of 20 ml/min (from room temperature to 650°C), at a ramp rate of 10°C/min. NH<sub>3</sub> desorption was measured using a thermal conductivity detector (TCD) and the total desorbed NH<sub>3</sub> was obtained from the integrated peak area of the TPD profiles relative to the calibration curve.

The surface morphology and localized metal concentration of the catalysts were determined by SEM-EDX analysis using a Carl Zeiss SMT EVO series scanning electron microscope. The sample preparation was done by mounting wafer form samples on the sticky carbon tape and electrically conducting by plating the sample with silver (20 nm thick) using a Bio-Rad Polaran sputter coater. Particle size of the calcined catalyst were analysed by Philips CM12 model Transmission Electron Microscopy

(TEM). The samples were prepared by ultrasonic dispersion of the calcined catalyst in methanol for 2 h and the sample was then dispersed onto a carbon copper grid. The X-ray diffraction patterns of all three calcined catalysts were examined using a Phillips X Pert Diffractometer PW 1390 at 40 kV and 30 mA on Cu K $\alpha$  radiation. The diffractograms were collected at  $2\theta$  between 10 to 80°. FT-IR spectra of HZSM-5, CAT-1, and CAT-2 catalysts were recorded in the vibrational region between 400 and 2000  $\text{cm}^{-1}$  with a PerkinElmer spectrum 100 infrared spectrometer using the conventional KBr disk technique. The catalyst sample was first dried at 350° for 2 h and the wafers were prepared with a ratio of catalyst : KBr = 1:100 under a pressure of 5  $\text{kg/cm}^3$ .

### 2.3 Catalytic Activity Test

The catalytic activity test was performed in a fixed bed reactor made up of quartz having internal diameter of 10 mm. The schematic diagram of the experimental set-up is shown in Figure1. Approximately 3g of catalyst (0.5 mm size) mixed with silicon carbide to avoid channeling was kept in the middle zone of the reactor. A K-type of thermocouple was placed near the catalyst bed to measure the temperature of the bed controlled by a PID controller.

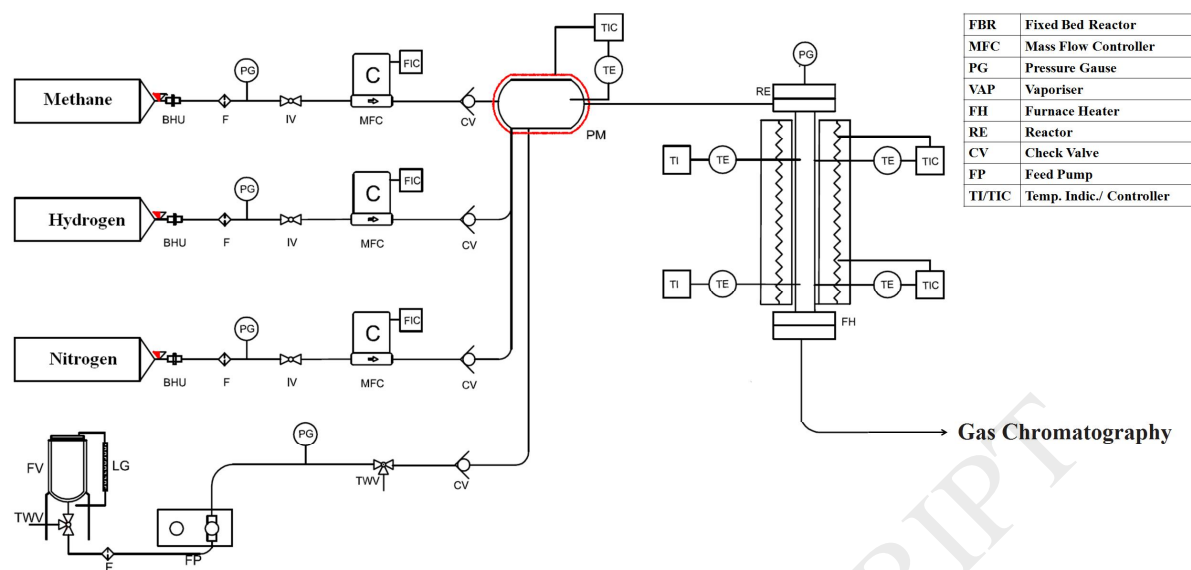


Figure 1. Experimental set-up for methane conversion

Prior to the catalytic test, the catalysts were first reduced in a stream of hydrogen and methane mixture (3:1) for 5 h, at a temperature of 460°C, which was predetermined through the TPR study. After reduction, the reactor was heated under nitrogen stream to the desired reaction temperature. Methane was introduced into the reactor through a calibrated mass flow controller. The gas hourly space velocity of methane was varied between 400 and 600 cm<sup>3</sup>/gh. The flow rate of methanol was 0.5 cm<sup>3</sup>/h for all cases. The flow rate of the product gases were measured by a soap bubble flow meter and the mixture components were analyzed by gas chromatography. The amounts of aliphatic and aromatic hydrocarbons were determined using FID-based gas chromatography equipped with Porapak-Q column. The methane conversion and selectivity were calculated on the carbon number basis. The conversion and selectivity are calculated by the following formula:

$$\text{Conversion(\%)} = \left( \frac{(\text{moles of CH}_4 \text{ fed} - \text{moles of CH}_4 \text{ out} + \text{moles of CH}_4 \text{ produced from methanol})}{\text{moles of CH}_4 \text{ fed}} \right) \times 100$$

(Methane produced from methanol under the same condition without methane addition in the feed)

$$\text{Selectivity} = \left( \frac{\text{Amount of product formed}}{(\text{moles of CH}_4 \text{ fed} - \text{moles of CH}_4 \text{ out} + \text{moles of CH}_4 \text{ produced from methanol})} \right) \times 100$$

### 3.0 Results and Discussion

#### 3.1 Surface Area and Pore Volume of Catalysts

The BET surface area, pore volume, average pore diameter of the parent zeolite (HZSM-5, Si/Al=55), and the other two bimetallic catalysts are given in Table 1. The data show that the surface area of catalyst decreased due to metal loading. The decrease in surface area with the increased metal concentration may be due to partial pore blockage during the impregnation of the Mo/Zn on the HZSM-5 which was also supported by the decrease in pore volume with the increase of metal concentration.

Table 1. BET surface area, pore volume, average pore diameter, and percentage metal dispersion of the support and catalysts.

| Composition      | Nomenclature | BET SA (m <sup>2</sup> /g) | Pore Volume (cm <sup>3</sup> /g) | Avg. Pore Diameter (Å) | Percent Metal Dispersion |
|------------------|--------------|----------------------------|----------------------------------|------------------------|--------------------------|
| H-ZSM-5          | H-ZSM-5      | 262.14                     | 0.36                             | 55.89                  | -                        |
| 5%Mo/HZSM-5      | CAT-1        | 250.49                     | 0.34                             | 55.01                  | 1.28                     |
| 5%Mo-2%Zn/HZSM-5 | CAT-2        | 236.01                     | 0.32                             | 724.39                 | 0.72                     |

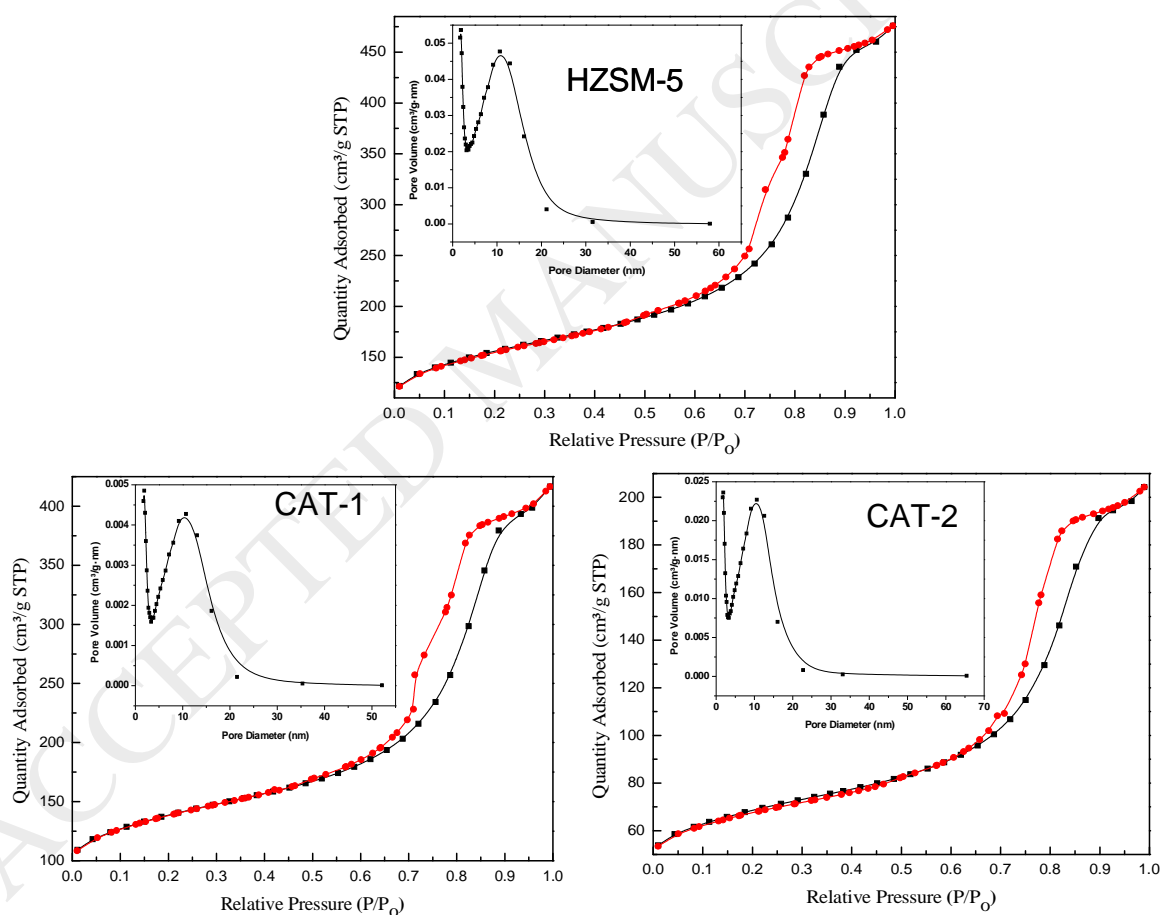


Figure 2. N<sub>2</sub> adsorption-desorption isotherm and BJH pore size distribution (inset) of the two catalysts.

Figure 2 shows the N<sub>2</sub> adsorption/desorption isotherms and pore size distribution of HZSM-5 and other two metal impregnated catalysts. Both isotherm showing a typical Type IV isotherm, with a capillary condensation at P/P<sub>0</sub> of 0.7–0.9 and a sharp rise in the gas uptake at higher relative pressure, signifying the presence of large mesopores. The BJH isotherm and pore volume distribution analyze indicate the presence of distinctive mesopores. For all of the catalyst samples, the effective diameters were almost equivalent to those of the original HZSM-5, which suggest that the metal has not much effect on pore size distribution. This could be the exchange of metal ions with protons of the H-ZSM-5 as a result of which metal particles are present at the outer surface as well as outside the channels and no pores were blocked. On the other hand, due to non-interference of the metal particles to the channels and pore openings of the H-ZSM-5, no significance difference has occurred in the pore size distribution of the base material and both the catalysts. According to the BJH calculation, the most of these mesopores and in the range of 2–21 nm, with a sharp maxima at about 11.5 nm (Figure 2, inset), indicating that the catalysts exist in the combined form of micro and meso porosity which is favoured from the mass transport point of view for methane conversion process.

### 3.2. TPR, Chemisorption, and TPD Analysis

To determine the reducibility of the calcined catalysts, temperature-programmed reductions were performed from ambient temperature to 950°C. Figure 3 shows the H<sub>2</sub>-TPR profile for the two catalysts, with two distinct peaks observed for each CAT-1 and CAT-2. The first peak appeared at the temperature range between 430-450°C, corresponding to the reduction of molybdenum species. The second peak significantly shifted to a higher temperature (~950°C), this is attributed either to the reduction of the

MoO nanoparticles being reduced to active Mo, or due to a strong interaction between MoO in the HZSM-5 framework reduced at higher temperatures [16]. There was no peak found at this temperature range for zinc oxide indicating that zinc oxide was not reduced within this temperature range which is in agreement with the literature [17, 18]

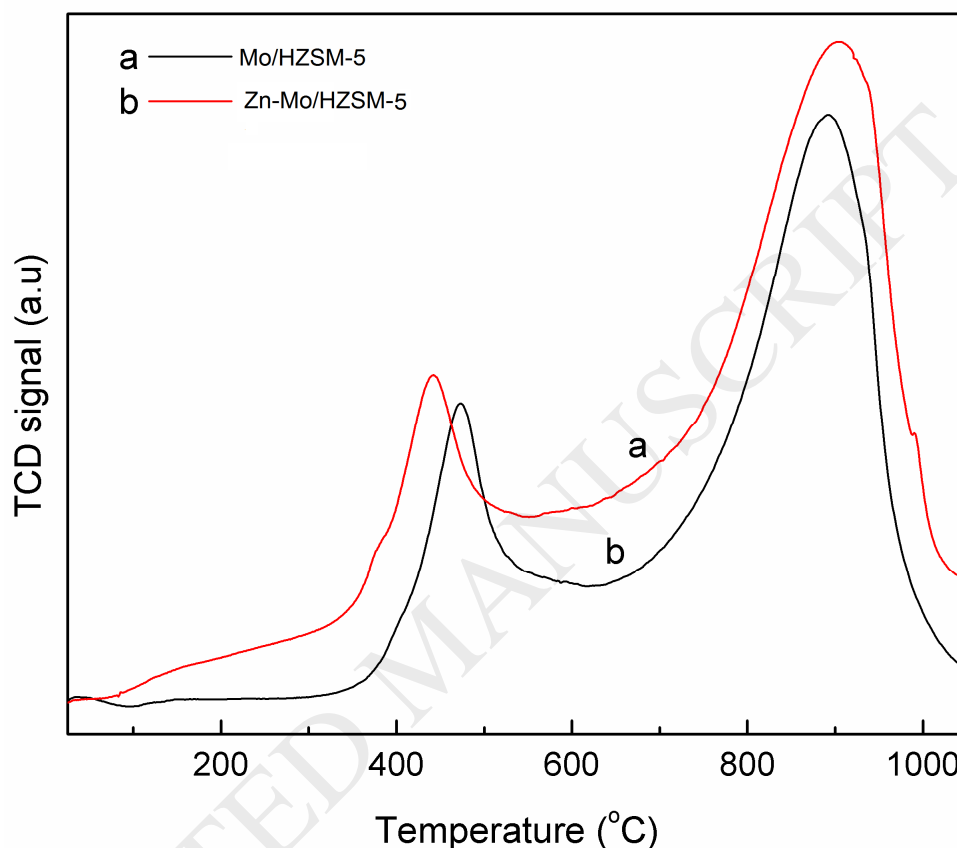


Figure 3. H<sub>2</sub>-TPR profiles of CAT-1 and CAT-2 catalyst.

The acidity of calcined catalysts were determined by NH<sub>3</sub>-TPD analysis. As shown in Figure 4, the NH<sub>3</sub>-TPD spectra of CAT-1 and CAT-2 resemble moderate acid sites. It has been reported that acid sites are classified as weak (<300°C), moderate (300~450°C), and strong (450~550°C), depending upon the desorption temperature [19]. Results indicate that presence of molybdenum into HZSM-5 decreases the strength of stronger acidic sites. Ma et al. reported that ammonia adsorbs

on both the weak (Lewis) and strong (Brönsted) acid sites. Incorporation of Mo and zinc in HZSM-5 slightly changed the acidic properties of the catalysts due to which catalyst loses some of Brönsted acid sites and, ultimately, forming Lewis acid sites. Two reasons behind the Lewis acid formation are: firstly, the migration of Mo into the zeolite channel and, secondly, the pore occupied by the access metal concentration inside the zeolite [20, 21].

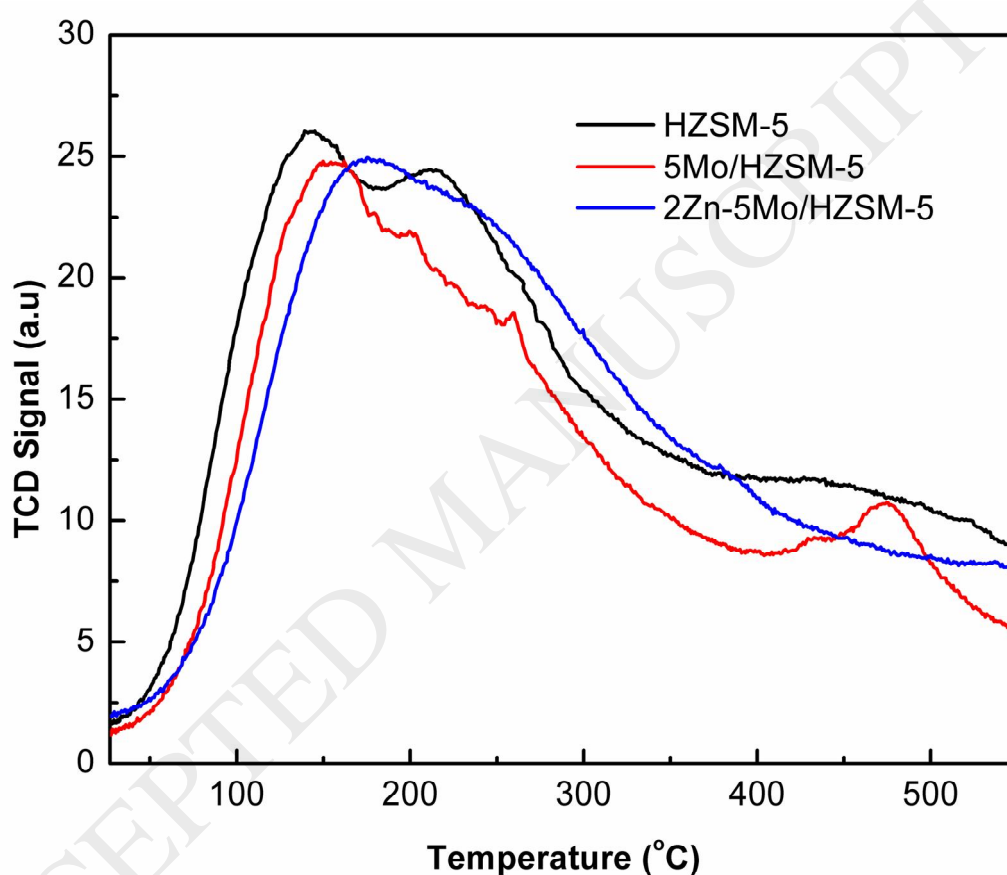


Figure 4. NH<sub>3</sub>-TPD profiles of CAT-1 and CAT-2 catalyst.

### 3.3 Catalyst Morphology

#### 3.3.1 XRD analysis

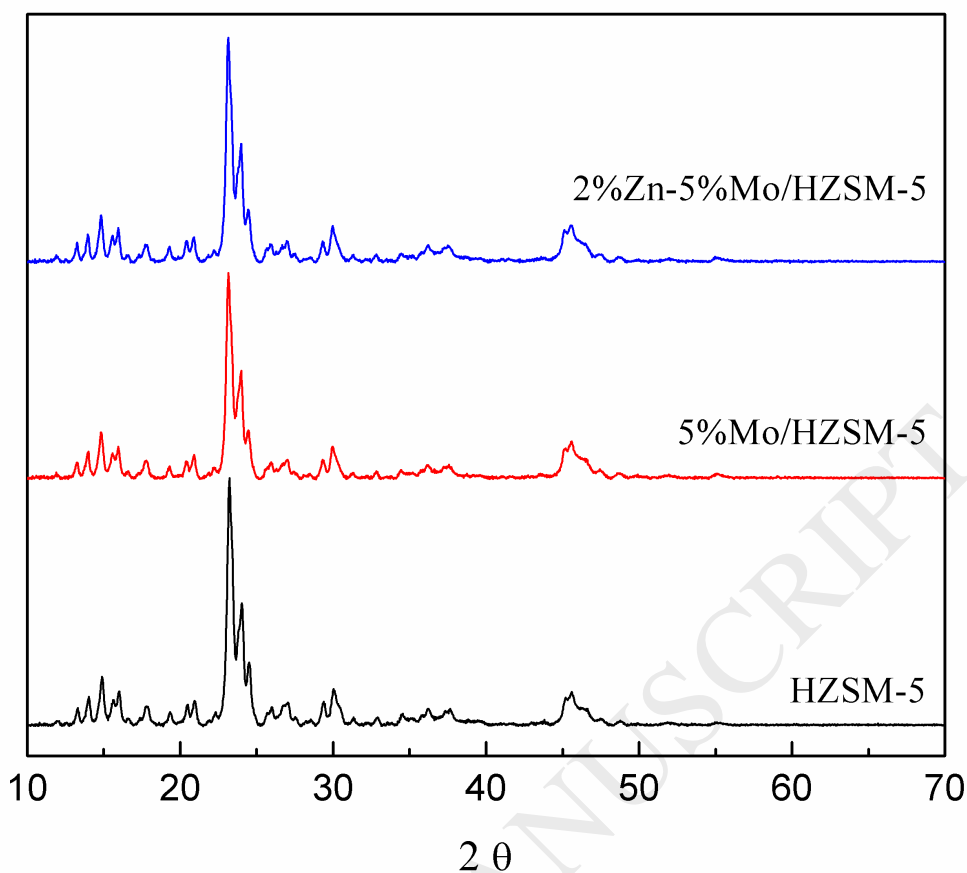


Figure 5. XRD analysis of HZSM-5, CAT-1, and CAT-2 calcined catalysts.

XRD technique was used for the identification of the phase of molybdenum and zinc oxide on the HZSM-5 support and their interaction. The diffraction peaks for HZSM-5, CAT-1, and CAT-2 (Figure 5) did not show any appreciable change in  $2\theta$  position, implying that there was no any phase change in the catalysts after the impregnation of Mo and Zn on HZSM-5. Also, no new XRD peaks were observed for the molybdenum and zinc species, indicating that Mo and Zn are highly dispersed on the HZSM-5 surface and/or in its framework. Xu et al.[22] explained that Mo species on HZSM-5 prepared by the impregnation method are generally well dispersed on the zeolite

surface and the crystal size of  $\text{MoO}_3$  and  $\text{Al}_2(\text{MoO}_4)_3$  below 4 nm cannot be detected by the XRD technique.

### 3.4 SEM-EDX and TEM analyses

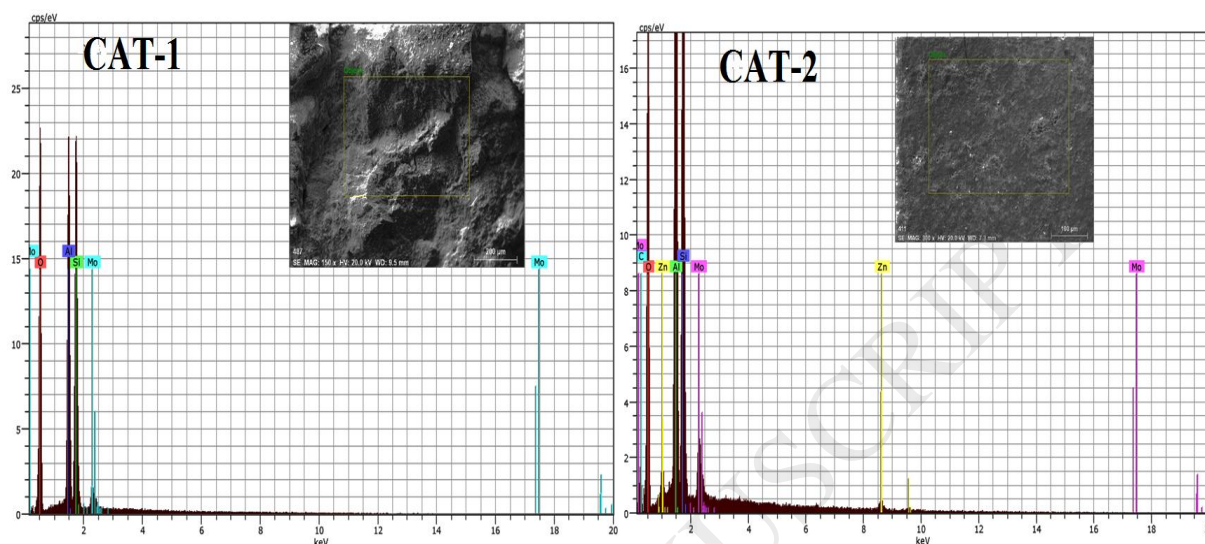


Figure 6: SEM-EDX analysis of CAT-1 and CAT-2.

The surface morphology of CAT-1 and CAT-2 was studied by SEM analysis. As shown in the SEM micrographs (Figure 6 inset), the particles are irregular in shape with uneven distribution and their size varied from 200–257  $\mu\text{m}$ . The average concentrations of Mo and Zn in the calcined CAT-1 and CAT-2 catalysts were analyzed by EDX analysis. Molybdenum was found to be less than of 4% whereas zinc for CAT-2, was 1.3%. These results are shown in Table 2 and the EDX elemental mapping for both catalysts is shown in Figure 6. From the data, it can be perceived that the Mo concentration for both catalysts is less than 4% and the Zn concentration is about 1.3% for CAT-2.

Table2. Elemental analysis of CAT-1 and CAT-2.

| Catalyst | Si (Wt %) | Al (Wt %) | O (Wt %) | Mo (Wt %) | Zn (Wt %) |
|----------|-----------|-----------|----------|-----------|-----------|
| CAT-1    | 18.8      | 19.2      | 58.4     | 3.6       | -         |
| CAT-2    | 17.6      | 16.8      | 60.9     | 3.4       | 1.3       |

TEM analysis was also used to determine the size and shape of the catalyst particles. From Figure 7, it can be seen that Mo particles are represented by the dark spots in the micrograph. The TEM images also showed clusters of metal particles with support, having an uneven distribution and being heterogeneously dispersed in an average cluster size of 20–100 nm.

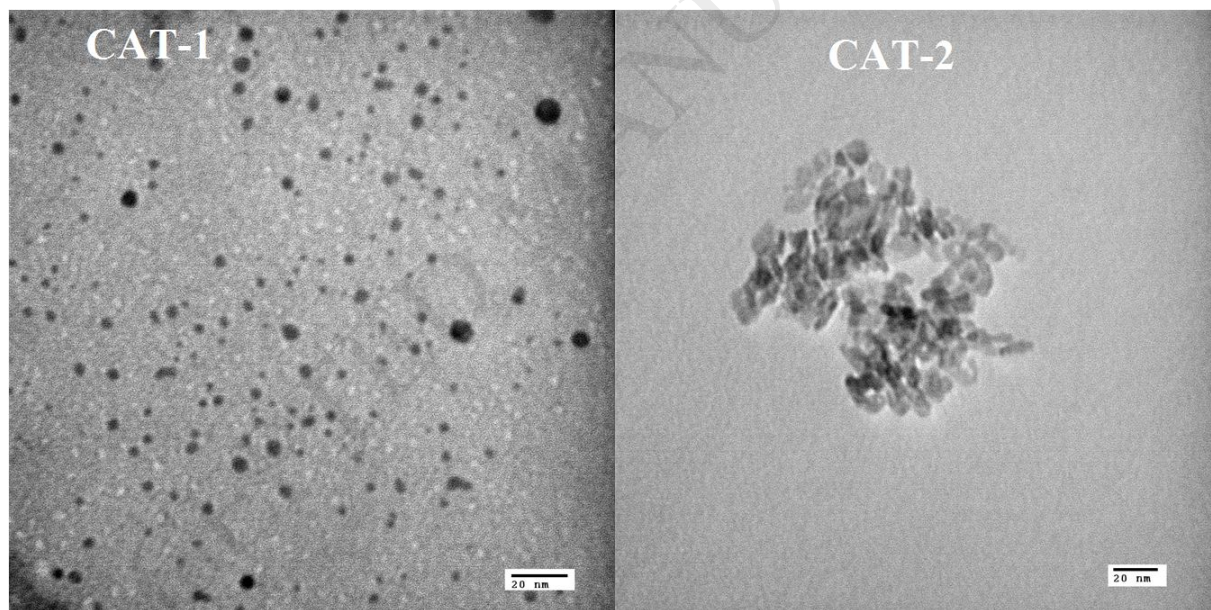


Figure 7. TEM analysis of CAT-1 and CAT-2 calcined catalysts.

### 3.5 FT-IR Analysis

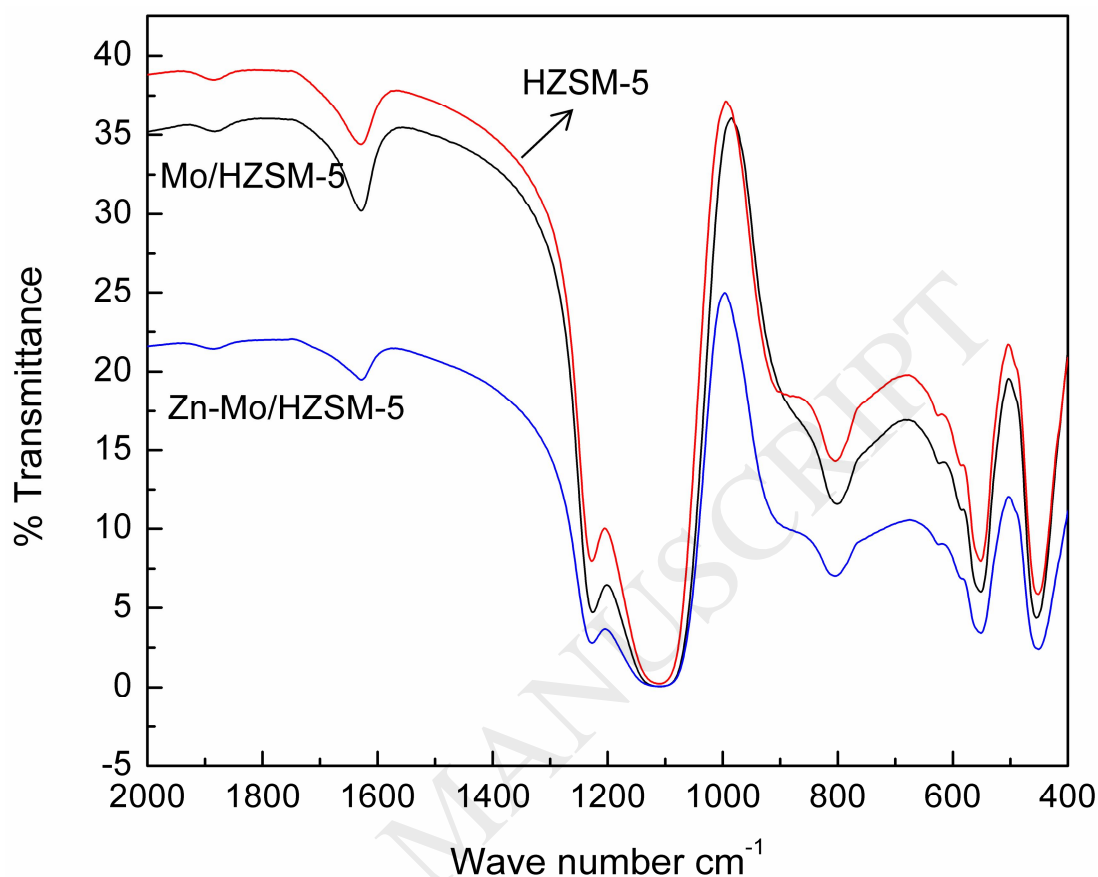


Figure 8. FTIR analysis of HZSM-5, CAT-1 and CAT-2 calcined catalysts.

The framework structure of HZSM-5 and the two catalysts were characterized by FT-IR analysis. The position of all the structure-sensitive bands in the IR spectra of the HZSM-5 zeolite and the two calcined catalysts are observed at the same position (Figure 8), which suggests that the basic zeolite structures are not affected much by the incorporation of Mo and Zn species. However, as indicated by the results of  $\text{NH}_3$  TPD (Figure 4), where  $\text{NH}_3$  is desorbed at temperatures in the range of 110-400°C (weak site range), it is interesting to note how the strong sites are converted into weak sites. The

absorption bands at 1222, 1100, 795, 547, and 453  $\text{cm}^{-1}$  are characteristic of the HZSM-5 framework [20]. Although both catalysts show similar bands at the same position, there is a difference in the decrease in intensity, suggesting that the loading of the metal species affect the bonding behavior in the zeolite framework.

### 3.6 Synthesis and Product Selectivity

It is widely accepted that the most promising catalyst for non-oxidative methane conversion is Mo/H-ZSM-5 [23]. By the incorporation of zinc on HZSM-5, some of the protons are replaced by zinc atom, which increases reaction rate. Iglesia et al. explained that the activation of C-H bond occur on protonic acid sites, but they recombine again with abundant surface hydrogen species, because protonic acid sites are not able to remove hydrogen via recombinative desorption. Zn cations can prevent these recombination reactions by providing a function for recombinative desorption and removing the hydrogen atoms formed during C-H activation [13]. Keeping those in mind effects of activation procedures on methane-methanol co-conversion were compared over the CAT-1 and CAT-2 catalysts. In our previous work, the effect of copper and zinc loading on HZSM-5 were studied for methanol to higher hydrocarbon conversion [23, 24]. It was found that the aromatics selectivity varied from 66 to 77%, rest were aliphatic hydrocarbon. In the same way in the present investigation methanol conversion was tested over CAT-1 and CAT-2 catalysts under the same reaction conditions as that of methane methanol co-conversion at 550 °C. Nitrogen was used to maintain methane partial pressure. Methanol was found to be 100% conversion for both the catalyst. The product selectivity are shown in Table 3 for methanol conversion on water free basis.

Table 3. The hydrocarbons product selectivity for the catalytic conversion of methanol over CAT-1 and CAT-2 at 550 °C. The data were taken at 1 h of time on stream.

| Selectivity               | CAT-1 | CAT-2 |
|---------------------------|-------|-------|
| Methane                   | 3.2   | 2.4   |
| Ethylene                  | 8.6   | 9.2   |
| Ethane                    | 1.6   | 1.8   |
| Propylene                 | 3.4   | 3.5   |
| Propane                   | 1.8   | 1.1   |
| Butylenes                 | 4.2   | 3.8   |
| Butane                    | 5.2   | 5.7   |
| Benzene                   | 9.2   | 7.8   |
| Toluene                   | 6.8   | 6.4   |
| C <sub>8</sub> aromatics  | 24.7  | 25.2  |
| C <sub>≥9</sub> aromatics | 31.3  | 33.1  |

The catalytic performances of co-conversion of methane with methanol over CAT-1 and CAT-2 catalysts at two GHSV were studied at three different temperatures for 5 h of reaction. Figure 8 shows the methane conversion with the time on stream. The results indicated that the methane conversion over CAT-2 is higher than CAT-1 where as methanol was completely reacted. The decrease in methane conversion with time on stream may be due to the carbonaceous deposition of methane/methanol over the catalyst. This is supported by the TGA analysis of the catalyst after the reaction (Figure 9). Zn has a significant contribution on the methane conversion. Table 4 and 5 shows the conversion results of effect of Zn on the reactivity of methane over catalysts CAT-1 and CAT-2.

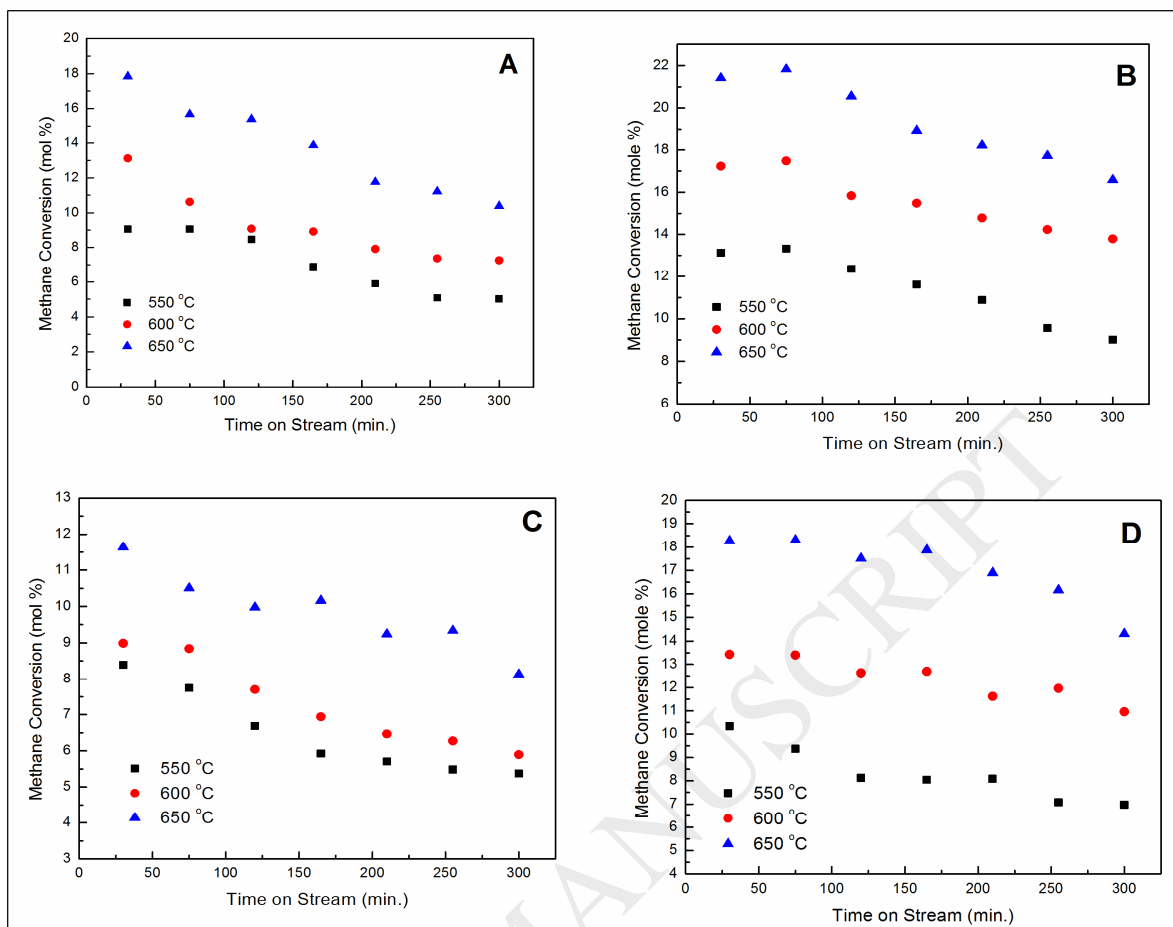


Figure 9. Catalytic methane conversion vs time on-stream on (A) CAT-1 at GHSV 400 ml/h.g<sub>cat</sub>, (B) CAT-2 at GHSV 400 ml/h.g<sub>cat</sub>, (C) CAT-1 at GHSV 600 ml/h.g<sub>cat</sub>, (D) CAT-2 at GHSV 600 ml/h.g<sub>cat</sub>.

From Figure 9, it can be revealed that there is a significant improvement in the catalytic performance after the incorporation of Zn. Table 4 and 5 shows the product selectivity distribution for CAT-1 and CAT-2. The main gaseous products of the reaction were ethylene, ethane, propylene, propane, butylenes and butane. The liquid product mainly contained benzene, toluene, ethyl benzene and xylene. Incorporation of zinc enhanced the selectivity towards aromatic range products. It can be seen that as the temperature increases the methane conversion and ethylene selectivity increased

remarkably. This may be due to the dominance of cracking reaction. At a lower temperature 550 °C, the selectivity of toluene and xylene is higher as compared higher temperature (600 and 650 °C). The alkylation reaction favored at lower temperature. At relatively higher temperature, the contribution of oligomerization was favored because of which coke reposition occurred on the catalyst. The high selectivity of aromatics indicates a high activity of HZSM-5 and high concentration on its surface of strong acid centers responsible for aromatization of methane and methanol. The shift of the reaction toward low selectivity when temperature increases may be due to plugging of zeolite channels and voids with coke deposits, which deteriorate the catalyst activity.

Table 4. The effect of temperature on product selectivity over CAT-1 and CAT-2 at a methane flow rate 400 cm<sup>3</sup>/g h for methane conversion. The data were taken at 1 h of time on stream.

| Selectivity               | CAT-1  |        |        | CAT-2  |        |        |
|---------------------------|--------|--------|--------|--------|--------|--------|
|                           | 550 °C | 600 °C | 650 °C | 550 °C | 600 °C | 650 °C |
| Ethylene                  | 7.95   | 11.64  | 12.83  | 5.32   | 8.79   | 8.45   |
| Ethane                    | 2.75   | 4.72   | 1.61   | 6.21   | 2.94   | 4.67   |
| Propylene                 | 1.26   | 0.97   | 1.37   | 1.14   | 1.30   | 0.53   |
| Propane                   | 1.42   | 0.83   | 0.62   | 1.01   | 2.00   | 3.93   |
| Butylenes                 | 0.56   | 1.87   | 2.60   | 0.77   | 0.45   | 0.71   |
| Butane                    | 1.87   | 0.38   | 0.00   | 0.20   | 0.50   | 0.46   |
| Benzene                   | 29.44  | 37.92  | 38.33  | 12.17  | 15.20  | 10.20  |
| Toluene                   | 23.68  | 10.16  | 5.00   | 29.65  | 19.92  | 10.71  |
| C <sub>8</sub> aromatics  | 20.71  | 16.96  | 21.22  | 37.62  | 28.00  | 21.74  |
| C <sub>≥9</sub> aromatics | 10.36  | 14.56  | 16.42  | 5.89   | 20.90  | 38.60  |

Table 5. The effect of temperature on product selectivity over CAT-1 and CAT-2 at a methane flow rate 600 cm<sup>3</sup>/g h for methane conversion. The data were taken at 1 h of time on stream

| Selectivity               | CAT-1  |        |        | CAT-2  |        |        |
|---------------------------|--------|--------|--------|--------|--------|--------|
|                           | 550 °C | 600 °C | 650 °C | 550 °C | 600 °C | 650 °C |
| Ethylene                  | 8.01   | 14.75  | 12.51  | 6.59   | 12.70  | 11.88  |
| Ethane                    | 3.93   | 1.73   | 1.52   | 3.33   | 3.83   | 1.89   |
| Propylene                 | 1.31   | 1.59   | 2.32   | 8.16   | 1.91   | 1.54   |
| Propane                   | 0.83   | 0.45   | 1.15   | 1.28   | 1.22   | 0.37   |
| Butylenes                 | 0.38   | 1.46   | 1.07   | 0.93   | 0.43   | 0.36   |
| Butane                    | 1.16   | 0.38   | 1.01   | 3.77   | 0.15   | 0.00   |
| Benzene                   | 32.12  | 23.73  | 21.36  | 27.97  | 25.50  | 21.88  |
| Toluene                   | 18.75  | 24.24  | 12.40  | 12.08  | 18.20  | 14.35  |
| C <sub>8</sub> aromatics  | 21.11  | 17.54  | 16.69  | 29.16  | 27.57  | 24.90  |
| C <sub>≥9</sub> aromatics | 12.40  | 14.13  | 29.96  | 6.72   | 8.49   | 22.83  |

### 3.7 TGA analysis of spent catalyst

Thermo gravimetric analysis (TGA) of spent catalyst (CAT-2) was done in a SDT Q600 thermal analyzer. TGA results are shown in Figure 9. The weight loss was about 7% for 550 °C, 8.5% for 600 °C and 11% for 650 °C. The reduction pattern indicates that between ambient and 150 °C variation in wt. percentage was approximately 5%, which indicates it might be due to the presence of moisture and volatiles matter deposited in the porous structure during the reaction. Above 150 °C, a rise in the peak indicates the different carbonaceous compounds decomposed with some accumulation of mass due to reaction in presence of oxygen.

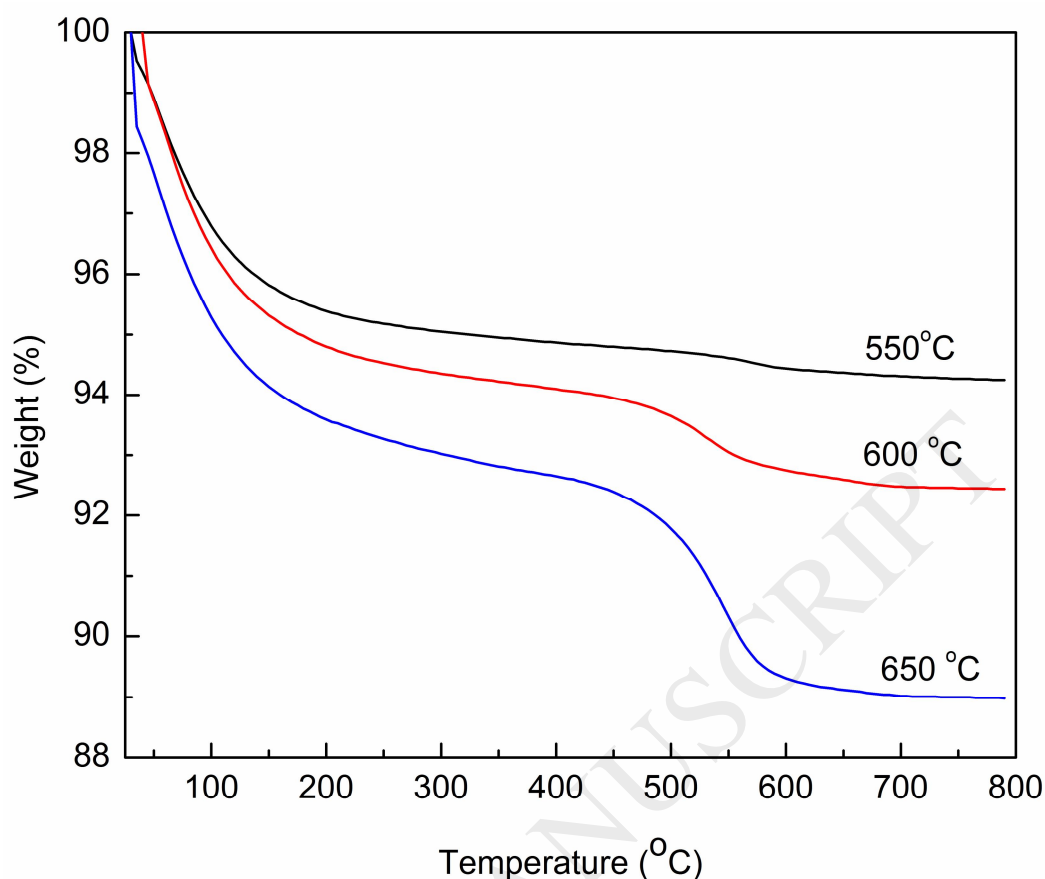


Figure 10. TGA profile of the spent CAT-2 catalyst (GHSV-400 ml/h.g<sub>cat</sub>)

#### 4.0 Conclusion

5%Mo/HZSM-5 (CAT-1) and 2%Zn-5% Mo/HZSM-5(CAT-2) catalysts were prepared by co-impregnation and tested for the co-conversion of methane with methanol at the condition of atmospheric pressure and three temperature (550, 600, and 650°C). It was found that the catalytic activity and selectivity of 5% Mo/HZSM-5 can be enhanced by the addition of Zn. A high methane conversion over the zinc-loaded Mo/HZSM-5 catalyst was found at a reaction temperature of 650°C; whereas, high selectivity was achieved at a reaction temperature of 600°C. BET surface area and pore volume were found to decrease in order when metal impregnation took place in HZSM-

5. The BJH isotherm and pore volume distribution analysis revealed the mesoporous nature of the catalyst. FTIR and XRD analyses suggested that the original framework remained the same, even after metal impregnation; whereas, the TPD results defined the moderate acidic nature of the catalyst.

ACCEPTED MANUSCRIPT

## References

1. J.F.Liu, Y. Liu, L.F.Peng, *J. Mol. Catal. A: Chem.* 280 (2008) 7
2. M.C. Alvarez-Galvan, N. Mota, M. Ojeda, S. Rojas, R.M. Navarro, J.L.G. Fierro, *Catal. Today* 171 (2011) 15.
3. J. H. Lunsford, *Catal. Today* 63 (2000) 165.
4. L. Wang, Y. Xu, S.T. Wong, W. Cui, X. Guo, *Appl. Catal. A: Gen.* 152 (1997) 173.
5. Y. Zhang, D. Wang, J. Fei, X. Zheng, *J. Nat. Gas Chem.* 12 (2003) 145.
6. V. R. Choudhary, A. K. Kinage and T. V. Choudhary *Chem. Commun.* (1996) 2545.
7. V.R. Choudhary, K.C. Mondal, S.A.R. Mulla, *Angew. Chem. Int. Ed.* 44(2005)4381.
8. P. Meriaudeau, L. V. Tiep, V.T.T. Ha, C.Naccache, G. Szabo, *J. Mol. Catal. A: Chem.* 144 (1999)469.
9. C. Bouchy, I. Schmidt, J.R. Anderson, C.J.H. Jacobsen, E.G. Derouane, S.B. Derouane-Abd Hamid, *J. Mol. Catal. A: Chem.* 163 (2000) 283.
10. W. Liu, Y. Xu, S.T. Wong, L. Wang, J. Qiu, N. Yang, *J. Mol. Catal. A: Chem.* 120 (1997) 257.
11. E.V. Matus, I. Z. Ismagilov, O.B. Sukhova, V.I. Zaikovskii, L.T. Tsikoza, Z. R. Ismagilov, *J.A. Moulijn, Ind. Eng. Chem. Res.* 46(2007)4063.
12. V.T.T. Ha, L.V.Tiepb, P. Meriaudeau, C. Naccache, *J. Mol. Catal. A: Chem.* 181 (2002) 283
13. E. Iglesia, D. G. Barton, J. A. Biscardi, M. J.L. Gines, S. L. Soled, *Catal. Today.* 38 (1997) 339.
14. C.L. Zhang, S. Li, Y. Yuana, W.X. Zhang, T.H. Wu, L.W. Catal. Lett. 56 (1998) 207.
15. A. A. Enein, A.L.H. Mahmoud, *Fuel* 90 (2011) 3040.
16. H. Jiang, L. Wang, W. Cui, Y. Xu, *Catal. Lett.* 57 (1999) 95.

17. M. M. Gunter, T. Ressler, R. E. Jentoft, B. Bems, *J. Catal.* 203 (2001)133.
18. W.F. Hoelderich, J. Tjoe, *Appl. Catal. A: Gen.* 184 (1999) 257.
19. J.R. Grzechowiak, J. Rynkowski, I. Wereszczako-Zielińska, *Catal. Today* 65 (2001) 225.
20. B. S. Liu, Y. Zhang, J. F. Liu, M. Tian, F. M. Zhang, C. T. Au, A. S. C. Cheung *115(2011)16954*.
21. L. Ovári, F. Solymosi, *J. Mol. Catal. A: Chem.* 207 (2004) 35
22. Y. Xu, W. Liu, S.T. Wong, L. Wang, X Guo, *Catal. Lett.* 40 (1996) 207.
23. Y. Xua, J. Wang, Y. Suzuki, Z.G. Zhang, *Catal. Today* 185 (2012) 41.
24. H.A. Zaidi, K.K. Pant, *Catal. Today* 96 (2004) 155.
25. H.A. Zaidi, K.K. Pant, *Ind. Eng. Chem. Res.* 47(2008) 2970.